Myo10 is a key regulator of TNT formation in neuronal cells.

Karine Gousset, Ludovica Marzo, Pierre-Henri Commere, Chiara Zurzolo

Myo10 is a key regulator of TNT formation in neuronal cells

Karine Gousset[1,*], Ludovica Marzo[1], Pierre-Henri Commere[2] and Chiara Zurzolo[1,‡]

[1]Institut Pasteur, 25 Rue du Dr Roux, Unité de Traffic Membranaire et Pathogenèse, 75724 Paris Cedex 15, France
[2]Institut Pasteur, 25 Rue du Dr Roux, Plate-Forme de Cytométrie en Flux, 75724 Paris Cedex 15, France
*Present address: Department of Biology, College of Science and Math, California State University, Fresno, 2555 East San Ramon Avenue M/S SB73, Fresno, CA 93740-8034, USA
‡Author for correspondence (chiara.zurzolo@pasteur.fr)

Summary

Cell-to-cell communication is essential in multicellular organisms. Tunneling nanotubes (TNTs) have emerged as a new type of intercellular spreading mechanism allowing the transport of various signals, organelles and pathogens. Here, we study the role of the unconventional molecular motor myosin-X (Myo10) in the formation of functional TNTs within neuronal CAD cells. Myo10 protein expression increases the number of TNTs and the transfer of vesicles between co-cultured cells. We also show that TNT formation requires both the motor and tail domains of the protein, and identify the F2 lobe of the FERM domain within the Myo10 tail as necessary for TNT formation. Taken together, these results indicate that, in neuronal cells, TNTs can arise from a subset of Myo10-driven dorsal filopodia, independent of its binding to integrins and N-cadherins. In addition our data highlight the existence of different mechanisms for the establishment and regulation of TNTs in neuronal cells and other cell types.

Key words: Myo10, TNTs, Dorsal filopodia, FERM domain, Intercellular transfer

Introduction

Cell-to-cell communication is vital for multicellular organisms. Almost a decade ago, Rustom and colleagues discovered new types of long-distance intercellular connections, called tunneling nanotubes (TNTs), allowing for the selective transport of membrane vesicles between cells (Rustom et al., Science. 2004). TNTs were described as long actin-rich tubular structures connecting distant cells that do not touch the substratum in culture (Rustom et al., Science. 2004). Since then, TNTs have been found in numerous cell types (Onfelt et al., 2006; Onfelt et al., 2004; Sowinski et al., 2008; Watkins and Salter, 2005, Wang et al. 2010; Lokar et al., 2010; Pasquier et al., 2013) enabling the transfer of signals, cytosolic materials and the spreading of pathogens (Sowinski et al., 2008; Gousset et al., 2009; Eugenin et al., 2009, Hase et al., 2009, Van Prooyen et al., 2010 Pasquier et al., 2013).

Tunneling nanotubes are very heterogeneous and numerous disparities have emerged both in their structures and functions (For reviews see Davis and Sowinski, 2008; Marzo et al., 2012). Some of these differences might arise from their mechanisms of formation. In the neuronal model cell line PC12, where they were first described, the principal means of TNT formation resulted from directed filopodia-like protrusions with a subset forming as a result of cell-to-cell detachment (Bukoreshtliev et al., 2009). Subsequently, formation resulting from cell-to-cell detachment was observed in numerous cell types, including immune cells (Onfelt et al., 2006; Onfelt et al., 2004; Sowinski et al., 2008; Watkins and Salter, 2005), and diverse cell lines, such as those derived from normal rat kidney cells, human embryonic kidney cells, neural crest cells and human primary umbilical vein endothelial cells (For review see Abounit and Zurzolo, 2012).

Both types of mechanism of formation can occur in the same cell type (Bukoreshtliev et al., 2009); however the molecular basis for their formation is still unclear. Recent studies have highlighted some early steps in TNT formation, such as the recruitment to the plasma membrane of the small GTPase RalA, filamin and the exocyst complex, by the transmembrane MHC class III protein LST1 (Schiller et al., 2012). This pathway, which also involves the known TNT inducer M-Sec (Hase et al., 2009), has been validated in immune cells, HeLa and HEK293T cells (Schiller et al., 2012). Other studies looking at stress-induced TNT formation in astrocytes point towards the involvement of p53 and the Akt/PI3K/mTor signaling pathways (Wang et al., 2011). However, no data are available concerning mechanisms of TNT formation in neuronal cells. For instance M-Sec appears restricted to myeloid lineages and neither microarray nor in situ hybridization experiments show its expression in neurons (personal communication; Hiroshi Ohno, RIKEN, Yokohama, Kanagawa, Japan). This implies that an M-Sec independent molecular mechanism must exist in neuronal cells. Furthermore, it is possible that different mechanisms of formation are involved in different cell types, and the predominance of one mechanism over the other could reflect the nature and functions of the cells. For example, mobile cells, such as immune cells, might readily form TNT-like structures using the cell-to-cell detachment mechanism, whereas immobile cells, such as neurons, might have to deploy actin-driven protrusions to reach distant cells.

Using CAD cells, a mouse neuronal cell line of catecholaminergic origin (Qi et al. 1997), we have previously shown that numerous TNT-like structures can be found in culture (Gousset et al., 2009). We have determined that these structures vary greatly both in lengths and diameters, and they contain actin

but not tubulin (Gousset et al., 2009). In addition, we have shown that they allow the transport of organelles, such as lysosomes and the spreading of infectious prion particles and proteinaceous aggregates (Gousset et al., 2009; Langevin et al., 2010; Costanzo et al., In Press). Since neuronal cells are mostly immobile, we hypothesize that TNTs in neurons arise from a specific subset of filopodia that are not attached to the substrate called dorsal filopodia (Bohil et al., 2006). A number of proteins, including the unconventional actin-based motor Myo10, vasodilator-stimulated phosphoprotein (VASP), fascin and the constitutively active mutant of Cdc42 were shown to induce dorsal filopodia in numerous cell types including COS-7, Hek-293 and neuronal CAD cells (Bohil et al., 2006). We focused our attention on Myo10 because it is widespread and expressed at low levels in different vertebrate tissues (Berg et al., 2000). Most importantly, in the brain Myo10 localizes in cell protrusions, including the tips of filopodia, and seems to be involved in the regulation of axonal outgrowth and cell migration (Berg and Cheney, 2002; Sousa et al., 2006, Raines et al., 2012).

Whereas the role of Myo10 in promoting substrate-attached filopodia has been extensively studied and requires binding to integrins (Zhang et al., 2004; Tokuo et al., 2007; Watanabe et al., 2010), much less is known about its role in dorsal filopodia (Bohil et al., 2006). Interestingly, during dorsal filopodia induction, Myo10 acts downstream of Cdc42 and is independent of VASP, another potent inducer of dorsal filopodia (Bohil et al., 2006) thus, demonstrating the existence of different mechanisms for dorsal filopodia formation.

The motor head domain of Myo10 allows the protein to move along the actin cables towards the tips of filopodia (Berg and Cheney, 2002). In addition, Myo10 contains a unique tail domain, which enables it to bind to a number of different proteins or lipids that are shown to have a role in filopodial extension (Zhang et al., 2004, Plantard et al., 2010, Umeki et al., 2011). The tail includes a PEST domain, three pleckstrin homology (PH) domains for binding to phosphatidylinositol $(3,4,5)$-trisphosphate $[PtdIns(3,4,5)P_3]$ (Plantard et al., 2010; Umeki et al., 2011), a myosin tail homology 4 (MyTH4) domain for binding to microtubules (Weber et al., 2004) and a band 4.1, ezrin, radixin, moesin (FERM) domain (Zhang et al., 2004) that interacts with the MyTH4 domain and is critical for binding to different cargoes (Wei et al., 2011, Hirano et al., 2011). While the FERM domain is composed of three subdomains (F1, F2 and F3 lobes), only the F2 and F3 lobes are required for Myo10 binding to integrins (Zhang et al., 2004). This domain is also important for binding to netrin receptors (Zhu et al., 2007) and to VE-Cadherins in endothelial cells (Almagro et al., 2010), suggesting that it is a general region for cargo binding. This hypothesis was further supported by recent structural studies (Wei et al., 2011, Hirano et al., 2011), showing that the netrin receptor DCC, integrins and microtubules bind to the same region (Hirano et al., 2011).

Here, we demonstrate that overexpression of Myo10 results in the formation of functional TNTs and in an increase of vesicle transfer between connected cells. Because other inducers of dorsal filopodia do not have this effect, we propose that in neuronal cells TNT formation arises from a specific subset of Myo10-dependent dorsal filopodia. We show that both the motor and tail domains of Myo10 are necessary for the induction of functional TNTs. Further analyses of tail mutants demonstrated that, whereas the PH2 domain is necessary, deletion of the F3

subdomain – a Myo10 integrin-binding site – does not affect TNT formation. This suggests that binding to PtdIns(3,4,5)P_3 but not to integrins is required for TNT formation, which further points at dorsal filopodia as the precursors of TNTs. Surprisingly, N-cadherins – previously shown to localize at TNT attachment sites (Lokar et al., 2010) and suitable Myo10 cargoes – are not likely to be involved because they do not colocalize with Myo10. However, we demonstrate that the F2 lobe of the FERM domain is necessary for Myo10-dependent TNTs. Finally, we show that the Myo10 pathway is not merging with the Akt pathway, which had previously been shown to induce TNT in astrocytes (Wang et al., 2011), supporting different regulations of TNT induction in different cell types.

Results

Myo10 increases the formation of TNTs

We have previously shown that, at steady state, about 40% of CAD cells are connected through TNTs, which vary greatly both in lengths and diameters (Gousset et al., 2009). Since these differences could derive from distinct mechanisms of formation, we analyzed the establishment of TNTs in CAD cells by live cell imaging. We observed that TNTs arise from extensions of filopodia as well as following cell-to-cell detachment (Fig. 1A,B and supplementary material Movies 1, 2). However, because neuronal cells are mainly immobile in the brain, we focused on the filopodia-driven mechanism (Fig. 1A and supplementary material Movie 1), which should be predominant in these cells. We hypothesized that dorsal filopodia are the precursors of this type of TNT and, therefore, analyzed whether known inducers of dorsal filopodia are involved (Bohil et al., 2006) in TNT formation. To this end, we transfected CAD cells with constructs encoding Myo10, VASP and fascin (Berg and Cheney, 2002; Adams and Schwartz, 2000) coupled to GFP, and quantified the number of formed TNT-like structures (supplementary material Fig. S1A-C). To characterize the effects of each protein in TNT induction, we displayed the relative percentage of cells with TNTs compared with control cells (Fig. 1C). Interestingly, overexpression of GFP-VASP and GFP-fascin decreased the ability of cells to form TNTs (Fig. 1C). Nevertheless, similar to what had previously been described (Bohil et al., 2006), GFP-VASP was found at the tips of filopodia (supplementary material Fig. S1E-b), and its overexpression increased dorsal filopodia (supplementary material Fig.S1D,E-a). However, for the majority of transfected cells, we observed recruitment of GFP-VASP to the sites of cell-to-cell adhesion, thus, increasing contact zones to levels not normally seen between CAD cells (supplementary material Fig. S1D,Ec,d). This change in the morphology of CAD cells resulted in a drastic decrease of TNT formation, with only 8.5% ($\pm$0.6) of the cells able to form TNTs compared with control cells (Fig. 1C).

By contrast, GFP-Myo10 increased the relative percentage of cells with TNT-like structures on average by >50% compared with control cells (Fig. 1C). TNTs induced by GFP-Myo10 overexpression were similar to those of control cells and only contained filamentous actin (data not shown). These data indicate that different types of filopodia exist and that filopodia-driven TNTs arise from a specific subset of dorsal filopodia that is Myo10-dependent. Furthermore, a mutant of Myo10 with a point mutation (KK1215/6AA) in the PH2 domain that blocks the binding of Myo10 to PtdIns(3,4,5)P_3 (Plantard et al., 2010), impaired its ability to induce TNTs (Fig. 1D). Thus, similar to

filopodia (Plantard et al., 2010, Umeki et al., 2011) the recruitment of Myo10 at the plasma membrane and its binding to PtdIns(3,4,5)P_3 appears to be necessary for TNT induction. Live image analyses showed the predominant presence of GFP-Myo10 within TNTs, and its back and forth movement over time (supplementary material Movie 3), reminiscent to the previously described intrafilopodial motility of Myo10 (Berg and Cheney, 2002). In addition, Myo10 overexpression resulted not only in an increase in the number of cells connected by tubular structures, but also in an increase in the number of TNTs observed between cells (Fig. 1E and supplementary material Movies 4, 5). Indeed, statistical analyses after counting and sorting cells that are connected by TNTs revealed that 46.8% ($\pm$2.9) of cells transfected with GFP-Myo10 formed three or more TNTs between cells, compared with 18.8% ($\pm$1.7) of control cells (Fig. 1F).

Myo10 overexpression increases the unidirectional transfer of vesicles

To determine whether Myo10-induced TNTs are functional (i.e. are active in vesicle transfer), we set up a flow cytometry assay to quantify the transfer of vesicles in our neuronal cell system, similar to what was previously described (Gurke et al. 2008; Bukoreshtliev et al., 2009). For these experiments, donor cells were loaded with the lipid dye DiD and mixed with CFP-transfected acceptor cells overnight (supplementary material Fig.
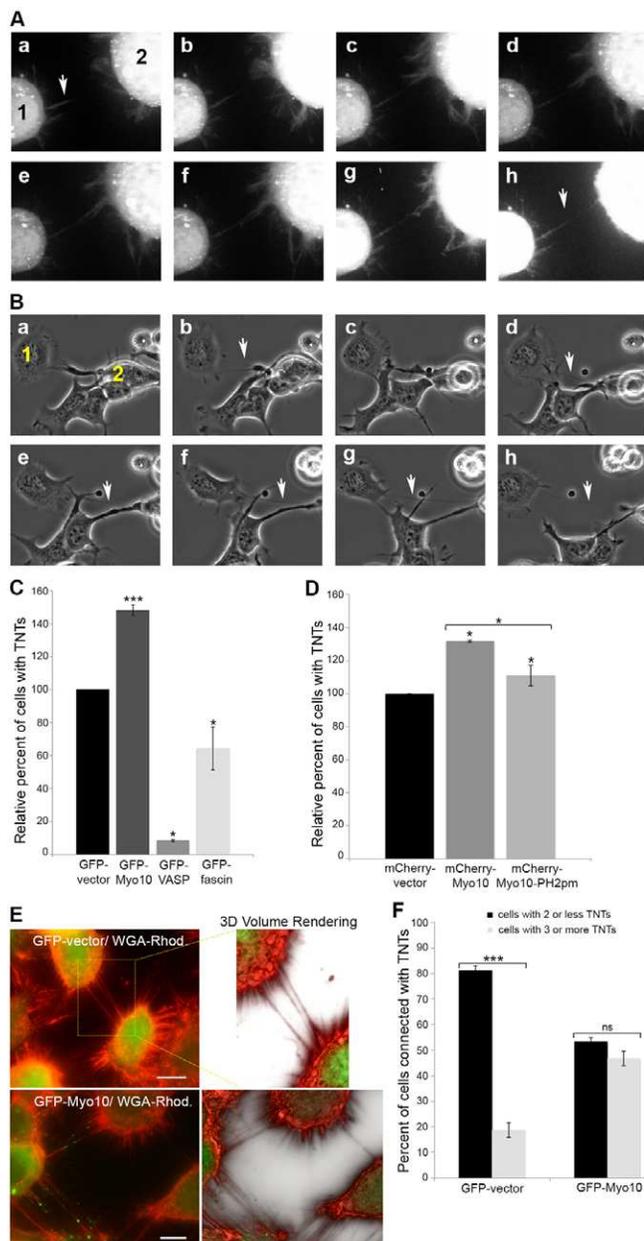

Fig. 1. GFP-Myo10 overexpression increases TNT numbers in neuronal CAD cells. (A) Filopodia-driven TNT formation. CAD cells were labeled with 5-carboxytetramethylrhodamine succinimidyl-ester (for membrane labeling) for 1 hour at 37°C and imaged live with a microscope confocal Revolution Nipkow spinning-disk imaging system (Andor Technology). Selected pictures were taken from supplementary material Movie 1 and put in a gallery to visualize the filopodia-driven mechanism of formation of a TNT. Over time (a-d) cell 1 extends a dorsal filopodia towards cell 2 (see arrow in a). Following filopodial interplay with cell 2 (e-f) and after attachment, the other filopodia from cell 2 retracts (g-h), generating a TNT (see arrow in h). This specific TNT was stable and was still present 2 hours after formation. The length of the movie is 40 minutes with time points taken every 30 seconds (see supplementary material Movie 1). (B) TNT formation following cell-to-cell detachment. Time-lapse analysis obtained with a Biostation IM from Nikon, phase-contrast images were taken every minute for 12 hours (see supplementary material Movie 2). Selected pictures were taken from supplementary material Movie 2 and put in a gallery to visualize TNT formation upon cell-to-cell detachment over time. In this example, cell 2 extends a large cell protrusion towards cell 1 (a and c) and, after contact and upon cell separation, multiple TNTs are visible between the two cells overtime (see arrows in b; d-h). (C) Effects of overexpression of dorsal filopodia inducers on TNT formation. CAD cells transiently transfected with GFP-vector (control), GFP-Myo10, GFP-VASP or GFP-fascin were fixed and labeled with the membrane dye WGA-Rhodamine in order to detect TNT structures, and the number of transfected cells connected with TNTs were counted. The relative percentage of TNT-connected cells upon overexpression of GFP-Myo10 (six independent experiments; n=701 cells), GFP-VASP (three independent experiments; n=364 cells) or GFP-fascin (three independent experiments; n=405 cells) compared with GFP-vector transfected cells (11 independent experiments, n=1304 cells) were evaluated. Overexpression of GFP- Myo10 greatly enhances TNT formation, whereas GFP-fascin hindered their establishment. GFP-VASP drastically inhibits TNTs, suggesting that TNTs specifically arise from Myo10-dependent dorsal filopodia. (D) Binding to PtdIns(3,4,5)P_3 is important for inducing TNTs. We determined the effects of a Myo10 construct with a point mutation in its PH2 domain (KK1215/6AA, mCherry-Myo10-PH2pm, n=225 cells), which blocks its binding to PtdIns(3,4,5)P_3, on TNT induction compared with mCherry-Myo10 (n=160 cells) and control mCherry-vector (n=144 cells). The PH2 mutant is not able to increase the number of TNTs to the levels of the full-length protein. Data are the average of three independent experiments. (E) Representative pictures of TNTs in control CAD cells (GFP-vector) on the top and GFP-Myo10 on the bottom. 3D projections obtained with OsiriX are presented on the right side of each original pictures. Cells transfected with both constructs are able to form TNTs but GFP-Myo10 expression induces multiple TNTs between cells compared with the control CADs. Scale bars: 10 µm (F) Quantification of the number of TNTs between transfected cells. The number of TNTs between cells was counted and the number of cells with two or less TNTs compared with the number of cells with three or more TNTs was plotted for both GFP-vector and GFP-Myo10 transfected cells. Upon overexpression of GFP-Myo10 , half of the cells with TNTs are connected with three or more TNTs, compared with overexpression of the GFP-vector, in which case over 80% of the cells connected have two or less TNTs between them. Data are the average of seven independent experiments. Graphs show means ($\pm$s.e.m.). *, see Statistical analyses under Materials and Methods; ns, not significant.

S2A). The amount of DiD-labeled vesicles transferred to the acceptor CFP-transfected cells was then quantified by flow cytometry (supplementary material Fig. S2B). As expected from our previous studies, control CAD cells transfected with GFP-vector can form functional TNTs (Gousset et al., 2009), allowing transfer of DiD vesicles from the donor cells to the acceptor cells that can be quantified by flow cytometry (supplementary material Fig. S2C-F, GFP-vector). Overtime, we observed cell-to-cell variability in the absolute number of vesicles transferring under control conditions (6–14%) (supplementary material Fig. S2C-F, GFP-vector). Thus, to compare different experimental conditions we displayed the relative transfer of DiD vesicles normalized to GFP-transfected donor cells – arbitrarily set at 100% (Fig. 2) as previously shown (Gurke et al., 2008). To understand whether the vesicle transfer observed in our experiments is the result of an active intercellular transfer mechanism, we first analyzed the transfer of vesicles obtained with fixed donor cells. As shown in Fig. 2A, no significant transfer of DiD-labeled vesicles was detected (Fig. 2A, Fixed; and supplementary material Fig. S2C), suggesting that vesicle transfer did not derived from the transfer of cell debris from the fixed donor population but requires an active mechanism. Next, to assess for the involvement of exosomes or membrane vesicles released within the medium, we incubated acceptor cells with the supernatant of GFP-vector donor cells. Under these conditions we detected only 28.8% (±3.7%) of transfer of DiD-labeled vesicles in acceptor cells, demonstrating that, in our setting, over 70% of the vesicle transfer requires cell-to-cell contact (Fig. 2A and supplementary material Fig. S2D). Significantly, when donor cells were transfected with GFP-Myo10 we observed a 1.4-fold increase in the relative transfer of DiD-labeled vesicles compared with control conditions (Fig. 2B and supplementary material Fig. S2E). It is important to note that, in contrast to the previous experiments where we specifically counted the number of TNTs

in CAD cells that express GFP-Myo10 (Fig. 1C), the flow cytometry experiments cannot discriminate between GFP-Myo10 transfected cells (20–30% transfection efficiency) and non-transfected cells. Thus, the 1.4-fold increase in vesicle transfer measured upon GFP-Myo10 transfection compared with control cells (Fig. 2B) is highly significant.

To further characterize the role of Myo10 overexpression on the transfer functionality of TNTs, we examined whether expression of Myo10 in donor or acceptor cells affects vesicle transfer. Thus, we analyzed the transfer of labeled vesicles from donor cells in co-culture, when only the acceptor cells were transfected with GFP-Myo10 (Fig. 2C and supplementary material Fig. S2F). Despite increasing the number of TNTs, overexpression of GFP-Myo10 in the acceptor cells had no effect on the transfer of vesicles from the donor population (Fig. 2C and supplementary material Fig. S2F). This suggests that, in CAD cells, the transfer of vesicles within Myo10-dependent TNTs is unidirectional, going from cells that created the tubes to acceptor cells.

Endogenous Myo10 is necessary for formation and function of TNTs

To assess whether Myo10 is required for TNT formation in CAD cells, we used Myo10 shRNA lentiviral particles to reduce the endogenous levels of Myo10 expression (Fig. 3A) and evaluated the effects on the number of TNTs. The number of cells with TNTs decreased by one-third when Myo10 expression was downregulated (Fig. 3B), indicating that Myo10 is required for the formation of a subset of TNTs in neuronal cells. Accordingly, in Myo10 knockdown cells the transfer of DiD-labeled vesicles was reduced to 78% (±4.2%) compared with control cells (Fig. 3C). Importantly, both the number of cells with TNTs (Fig. 3B) and the transfer of vesicles (Fig. 3C) were rescued upon overexpression of GFP-Myo10, demonstrating the
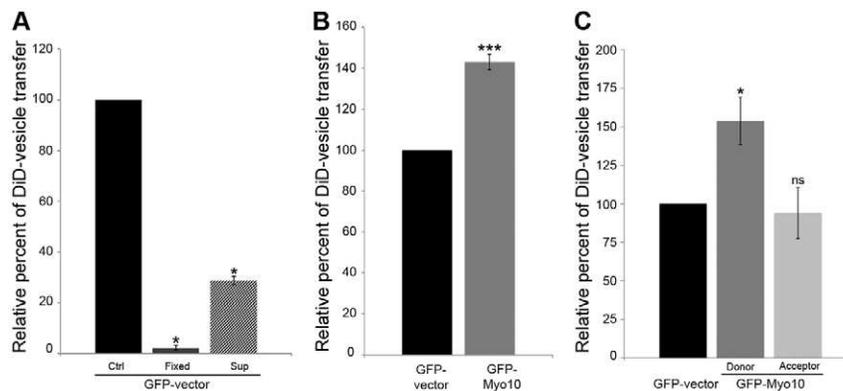

Fig. 2. Overexpression of Myo10 increases unidirectional transfer of DiD-labeled vesicles from donor to acceptor cells and needs cell-to-cell contact. To account for the variability in the absolute transfer of vesicles between experiments (supplementary material Fig. 2C-F), we normalized our data to the GFP-transfected control cells that we arbitrarily set at 100%. The relative percentage of transfer is presented for the each experimental condition. (A) The majority of vesicle transfer requires cell-to-cell contact and an active mechanism. CAD cells transiently transfected with GFP-vector are able to transfer DiD-labeled vesicles to acceptor cells. This transfer is highly restricted upon fixation of the donor cells and less than 30% of the vesicles are transferred through the medium. These data are consistent with an active, cell-to-cell-dependent mechanism and correlates with the presence of TNTs within the cultures. These data are the average of three independent experiments. (B) GFP-Myo10 overexpression in donor cells significantly increases the transfer of DiD-labeled vesicles compared with GFP-vector-transfected cells, suggesting that Myo10 induces TNT formation. These data are the average of 18 independent experiments. (C) GFP-Myo10 overexpression increases the transfer of DiD-labeled vesicles only when overexpression takes place in the donor cells. This suggests that the transfer of vesicles is unidirectional and goes from the cells that create the tubes to the acceptor cells. These data are the average of three independent experiments. Graphs show means (±s.e.m.). *, see Statistical analyses under Materials and Methods; ns, not significant.
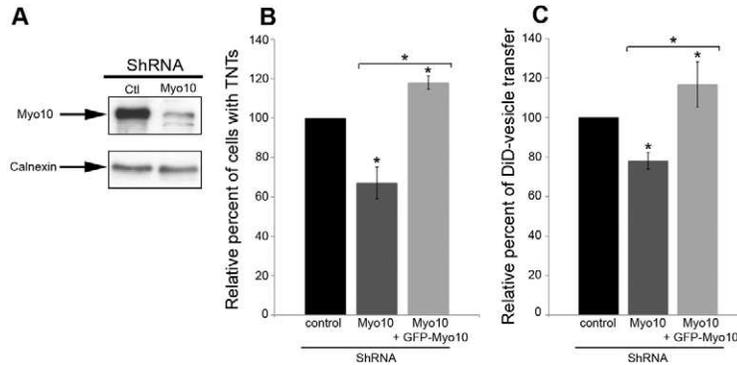
Fig. 3. Endogenous expression of Myo10 is necessary for TNT formation in CAD cells. (A) The endogenous levels of Myo10 were downregulated using Myo10 shRNA lentiviral particles. (B) Downregulation of Myo10 results in a decrease in the number of TNTs in CAD cultures. The relative percentage of cells connected by TNTs in Myo10-downregulated cells ($n=456$) compared with CAD cells treated with scramble shRNA lentiviral particles as control ($n=425$) was evaluated. The ability of Myo10-downregulated cells to form TNTs decreases by one-third compared with control cells. The relative percentage of cells connected by TNTs in Myo10-downregulated cells transfected with GFP-vector (control; $n=272$) can be rescued by overexpression of GFP-Myo10 ($n=240$). (C) In correlation with the presence of TNTs observed by microscopy, flow cytometry analysis shows that the relative percentage of DiD-labeled vesicles transferred in Myo10-downregulated cells decreases compared with the control cells. This defect in vesicle transfer can be rescued by overexpression of GFP-Myo10. Overall, these experiments show that Myo10 expression is able to induce a subset of TNTs in neuronal cells, directly affecting their intercellular ability. Data represent the average of at least three independent experiments. Graphs show means ($\pm$s.e.m.). *, see Statistical analyses under Materials and Methods: ns, not significant.

specificity of the Myo10 effect on TNT formation and function. It is important to note, however, that upon Myo10 knockdown the loss of TNTs was not complete. These results may reflect incomplete Myo10 knockdown (Fig. 3A) but, most probably, point towards the existence of Myo10-independent pathways for TNT formation – as previously described in different cell types (for review see Abounit and Zurzolo, 2012). This is also in agreement with our current observations that, in CAD cells, TNTs ensue from filopodia-protrusions as well as following cell-to-cell detachment (Movie 1, 2).

Full-length Myo10 is necessary for formation and function of TNTs

As mentioned before, the Myo10 motor domain is required for movement of Myo10 towards the tips of filopodia, whereas the tail is required for binding of Myo10 to factors necessary for filopodia elongation (Berg and Cheney, 2002; Zhang et al., 2004, Plantard et al., 2010, Umeki et al., 2011). To determine the role these domains might play in both TNT formation and function, we used two Myo10 mutants: GFP-HMM-Myo10, consisting of the head motor domain, neck and coiled-coil region of Myo10, and GFP-Myo10-Headless, containing the neck, coiled-coil and tail regions of Myo10 (Berg and Cheney 2002). We expressed both deletion mutants in CAD cells and analyzed their localization and effects on TNTs compared with the full-length protein. As previously described (Berg and Cheney, 2002), GFP-HMM-Myo10 is able to localize at the tips of filopodia, whereas GFP-Myo10-Headless is cytosolic (supplementary material Fig. S3A). Interestingly, and in contrast to the full-length protein (Fig. 1C,E,F), both mutants were unable to increase the relative number of cells with TNTs (Fig. 4A) or to create multiple TNTs between cells (Fig. 4B,C and supplementary material Movies 6-9). These data suggest that the localization of Myo10 at the tips of filopodia and its ability to move within TNTs is not enough to enhance TNT formation, and suggest that the tail domain of the protein is also required. In agreement with these findings, we found that, alone, neither construct can increase the transfer of

DiD-labeled vesicles to levels observed with GFP-Myo10 overexpression (Fig. 4D). These data highlight the correlation described above between the number of TNTs in cells in culture and the increase in the transfer of DiD-labeled vesicles, thus further identifying TNTs as an important vesicle-transport structure between neuronal cells.

Recently, it has been proposed that the headless form of Myo10 functions as a dominant regulator of full-length Myo10 because it suppresses the filopodia-inducing activity of full-length Myo10 upon coexpression in COS-7 cells (Raines et al., 2012). Thus, we checked whether this also occurs with TNTs, and co-transfected CAD cells with GFP-Myo10-Headless and mCherry-Myo10. Under these conditions, we observed that some of the headless protein relocalized from the cytosol (supplementary material Fig. S3A) to the tips of filopodia, together with the full-length protein (supplementary material Fig. S3C). However, in these cells we did not observe any reduction in the number of cells with TNTs compared with controls (cells coexpressing mCherry-Myo10 and GFP-vector) (Fig. 4E). Thus, in contrast to what was observed with substrate-attached filopodia, the headless form is not a dominant regulator of TNT formation, suggesting that the mechanisms by which Myo10 induces substrate-attached filopodia and TNTs are different and/or differently regulated.

The F2 subdomain of the FERM domain of Myo10 is required for formation and function of TNTs

To better characterize the mechanism of Myo10-mediated TNT induction, we decided to further investigate the role of the tail domain, which we found to be essential both for the formation of TNTs and for the transfer of labeled vesicles (Fig. 4A,D). To this end, we used two previously described Myo10 mutants, GFP-Myo10-ΔF2 and GFP-Myo10-ΔF3 that, respectively, lack the F2 or F3 lobes of the FERM domain located at the end of the Myo10 tail (Zhang et al., 2004). The F2 and F3 lobes of the FERM domain are necessary for integrin binding and for the elongation of attached filopodia (Zhang et al., 2004; Watanabe et al., 2010)

but not for the induction of dorsal filopodia (Bohil et al., 2006). In agreement with previous results both mutants localized at the tips of filopodia, similar to full-length GFP-Myo10 (Zhang et al., 2004), and were found within TNTs (supplementary material Fig. S3B; Fig. 5A and Movies 10, 11). Furthermore, like the full-length protein, GFP-Myo10-ΔF3 increased the number of cells

with TNTs and the number of TNTs between cells (Fig. 5B,C). Consistently, flow cytometry experiments showed that GFP-Myo10-ΔF3 also enhanced the transfer of DiD-labeled vesicles to levels similar to those of GFP-Myo10 (Fig. 5D), demonstrating that the F3 lobe is not required for TNT formation. By contrast, GFP-Myo10-ΔF2 was unable to increase TNT formation
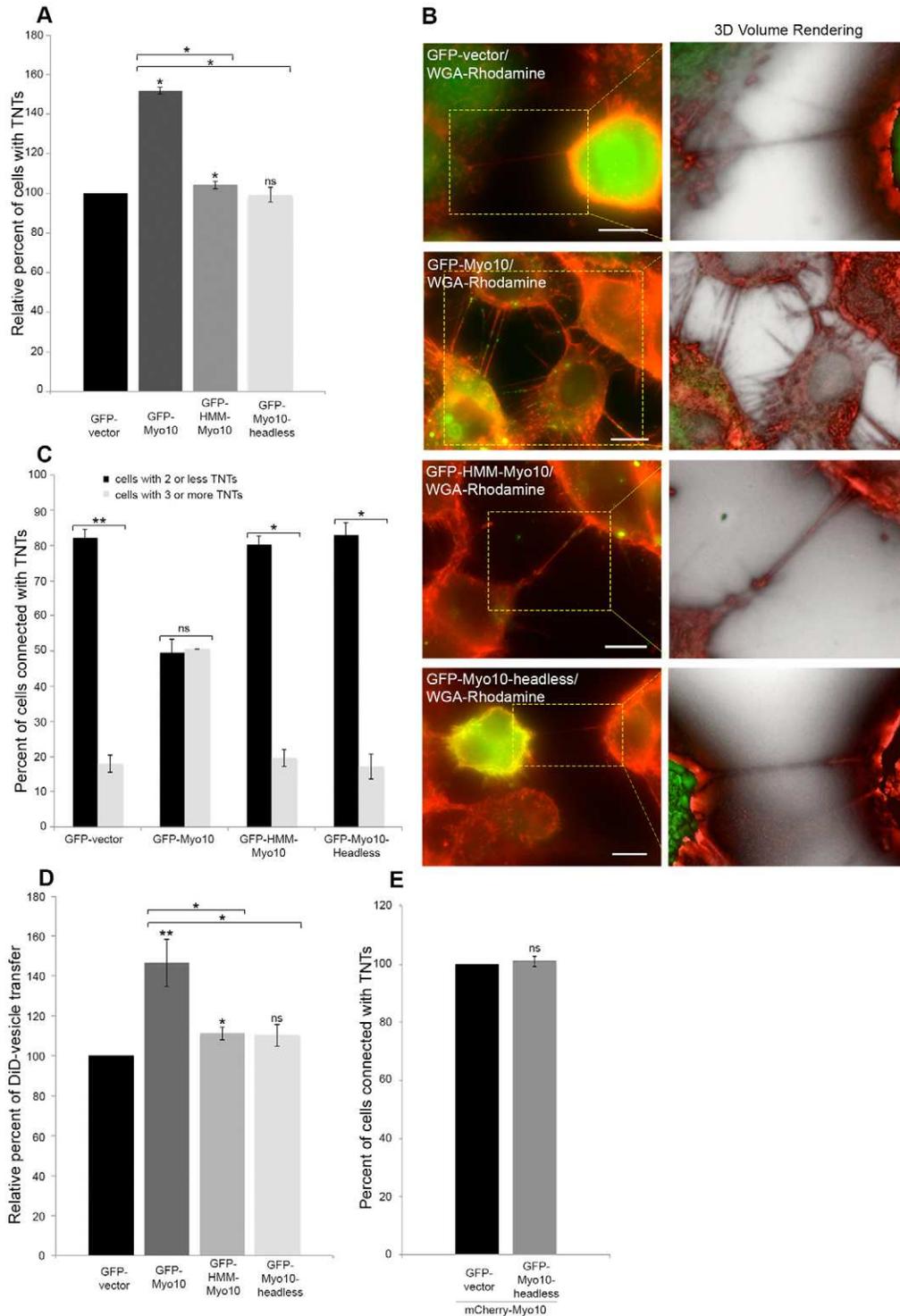
Fig. 4. See next page for legend.

(Fig. 5B,C) and the transfer of DiD-labeled vesicles (Fig. 5D). The fact that the Myo10 construct that lacked the entire FERM domain was still able to induce dorsal filopodia (Bohil et al., 2006) is in sharp contrast to the inability of the GFP-Myo10-ΔF2 mutant to increase functional TNTs, and indicates that the F2 lobe of the FERM domain is specifically required for the formation of Myo10-dependent TNTs in neuronal cells.

A recent study in an urothelial cell line proposed that N-cadherins has a role in TNT formation in that it provides attachment sites to neighboring cells (Lokar et al., 2010). In addition, in subconfluent human umbilical vein endothelial cells (HUVECs) (Almagro et al., 2010), Myo10 has been shown to mediate the transport of vascular endothelial-cadherins (VE-Cad) within filopodia to the cell edges that are necessary for the correct formation of cell–cell junctions. These independent observations led us to propose that N-cadherin is a downstream binding partner of Myo10. Thus, we coexpressed mCherry-Myo10 and GFP-N-cadherin in CAD cells, and analyzed their localization in subconfluent cells. However, we rarely found GFP-N-cadherin within filopodia and only little colocalization with Myo10 was observed (Fig. 5E), suggesting that other partners must be involved in Myo10-induced formation of TNTs in neuronal cells.

Myo10 expression regulates the formation of TNTs in neuronal cells in an Akt-pathway-independent manner

A recent study suggested that as a result of stress conditions, such as serum starvation or oxidative stress, TNTs are induced by p53 and Akt activation in astrocytes (Wang et al., 2011). However, this was not investigated in neuronal cells. Moreover, Akt has been implicated in the regulation of myosin 5a activity by increasing its interaction with F-actin and the transport of GLUT4 vesicles (Yoshizaki et al., 2007). Although, in contrast to myosin 5a, Myo10 is not a known vesicle carrier, we decided to explore whether in neuronal cells there is a link between these two mechanisms of TNT formation. First, we analyzed whether Myo10-dependent TNT formation activates the Akt signaling pathway. In neuronal cells, neither Myo10 downregulation (Fig. 6A) nor Myo10 overexpression (Fig. 6B) led to a major decrease or increase in endogenous Akt expression or Akt phosphorylation levels. These data suggest that the induction of Myo10-dependent TNTs in CAD cells is distinct from the TNT formation observed in astrocytes under stress conditions.

Next, we analyzed whether oxidative stress induced TNTs in CAD cells and whether this is directly linked to the activation of Akt. Similar to what had been described previously (Wang et al., 2011), treatment with H_2O_2 led to a drastic increase in the number of cells with TNTs, with almost 70% of CAD cells connected (Fig. 6C). However, western blot analyses revealed no increase in the levels of endogenous Akt and Akt phosphorylation in these cells (Fig. 6D). Thus, in contrast to what had been shown in astrocytes (Wang et al., 2011), TNTs that formed in neuronal cells following treatment with H_2O_2 are not the result of activation of the Akt signaling pathway (Fig. 6D). These data further demonstrate the existence of distinct mechanisms of TNT formation in different cell types, even when a similar stimulus is applied (in this case oxidative stress).

Discussion

The data presented here, on filopodia-driven TNT formation and the subsequent intercellular transfer of vesicles, identify the unconventional molecular motor Myo10 as a critical inducer of TNTs in neuronal cells. Here, we show that a number of similarities and differences exist between Myo10-dependent TNTs and filopodia, and propose that a specific subset of Myo10-dependent dorsal filopodia are the precursors of TNTs in neuronal cells. Similar to filopodia (Plantard et al., 2010, Umeki et al., 2011), the PH2 domain is required for Myo10 activity in promoting TNTs (Fig. 1D). This suggests that recruitment of Myo10 to the plasma membrane through PtdIns(3,4,5)P_3, which activates the motor allowing binding to cargoes and movement to the tips of filopodia (Umeki et al., 2011), is also required in the case of TNTs. Likewise, using deletion mutants, we show that neither the head nor the tail domains are sufficient to induce the formation of functional TNTs, and only overexpression of full-length Myo10 resulted in a substantial increase in functional TNTs in our cell cultures. However, in contrast to dorsal filopodia (Bohil et al., 2006), we demonstrated that the F2 lobe of the FERM domain is critical for TNT induction.

FERM domains link cytoskeletal components and integral membrane proteins. During filopodia elongation, Myo10 binds to integrins through the F2 and F3 lobes of its FERM domain, and brings them to the tips of filopodia creating adhesive platforms (Zhang et al., 2004). However, Myo10-induction of dorsal filopodia is integrin-independent and does not require the FERM domain (Bohil et al., 2006). We show here that, in the case of TNTs, the F3 deletion mutant mirrors full-length Myo10, thereby demonstrating clearly that the F3 lobe is not required for TNT formation and vesicle transfer. The F2 deletion mutant, by contrast, is inactive, which demonstrates that this lobe is essential. This suggests that, in contrast to attached-filopodia, Myo10-dependent TNTs do not need to bind to integrin. Most importantly, the F2 and F3 deletion mutants allowed the distinction between dorsal filopodia and TNTs, the latter of which specifically require the F2 lobe.

The function of the F2 lobe of the FERM domain of Myo10 is not clear. Structural studies have shown that the F2 lobe is unique

Fig. 4. Full-length Myo10 is necessary for functional TNTs. The roles of the motor or the tail domains of Myo10 on the induction of TNTs were assessed. CADs cells were transiently transfected with GFP-vector (control), GFP-Myo10, GFP-HMM-Myo10 (motor domain) and GFP-Myo10-Headless (tail domain), and fixed and labeled with the membrane dye WGA-Rhodamine in order to detect TNTs. (A) Only overexpression of full-length GFP-Myo10 (n=331) increases the number of TNTs compared with the GFP-vector control cells (n=660), GFP-HMM-Myo10 (n=484) or GFP-Myo10-Headless (n=385). The levels of transfections for these constructs range from 60–70% for GFP-vector, 20–30% for GFP-Myo10 and GFP-Myo10-Headless and 40–50% for GFP-HMM-Myo10. Data are the average of at least four independent experiments. (B) Representative pictures of TNTs in the different transfected cells are shown, together with 3D projections obtained using OsiriX. Scale bars: 10 μm. (C) The number of TNTs between cells was counted and plotted for all conditions. Only full-length GFP-Myo10-expressing cells are able to form numerous multiple TNTs compared with the other constructs. These data are the average of at least four independent experiments. (D) Flow-cytometry experiments show that GFP-Myo10 greatly enhances the transfer of DiD-labeled vesicles upon overexpression compared with control cells and GFP-HMM-Myo10 and GFP-Myo10-Headless. These data are the average of five independent experiments. (E) The Headless isoform does not regulate the ability of Myo10 to increase TNTs. CAD cells were co-transfected with mCherry-Myo10 and GFP-vector (control) or with GFP-Headless, fixed and labeled with the membrane dye WGA-Rhodamine in order to detect and count TNTs between transfected cells. We observed no differences in the induction of TNTs when GFP-Headless was coexpressed compared with GFP-vector control cells. Graphs show means (±s.e.m.). *, see Statistical analyses under Materials and Methods; ns, not significant.
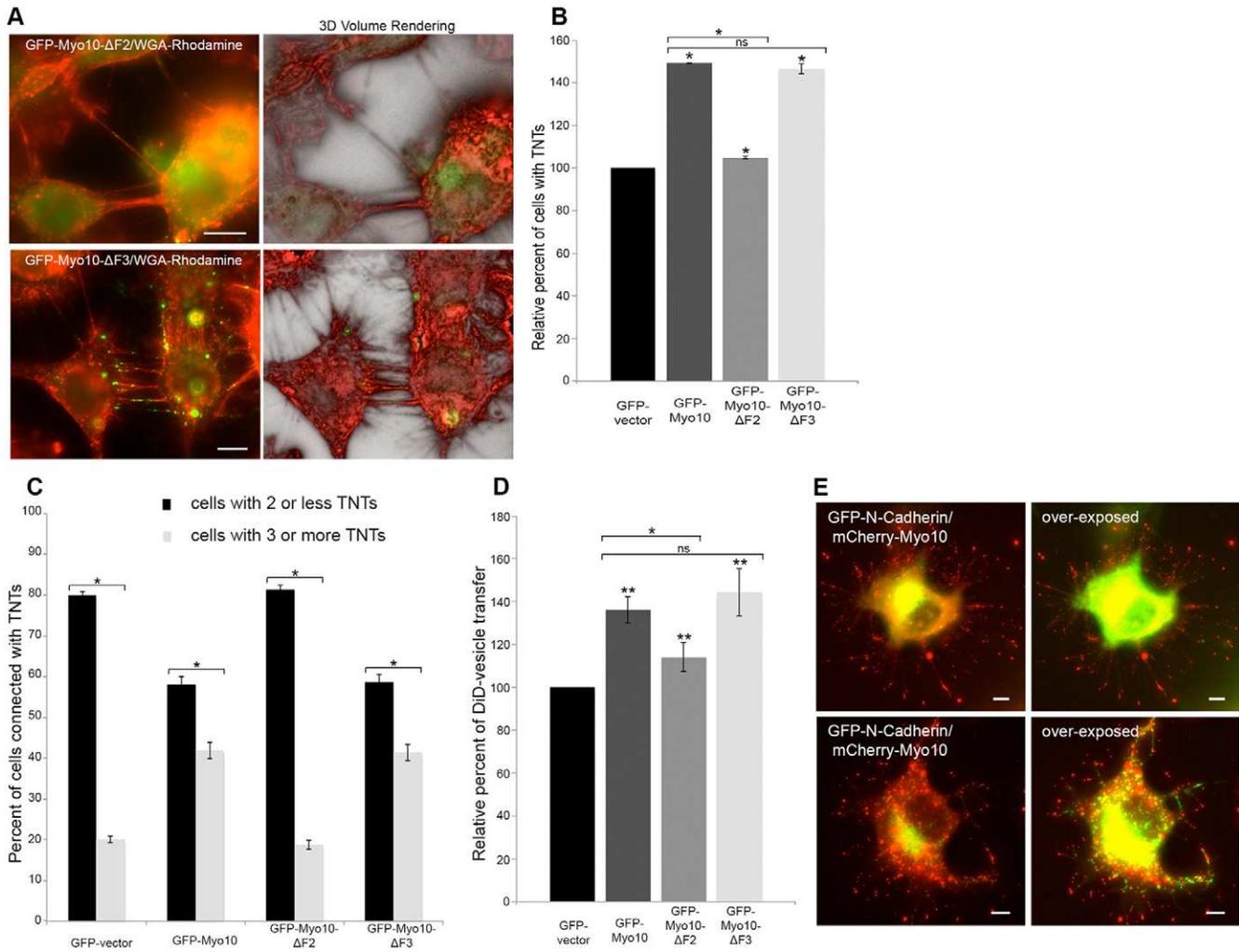
Fig. 5. The F2 subdomain of the FERM domain is required for functional TNT formation. (A) Representative images and 3D projections (OsiriX) of CADs cells transiently transfected with GFP-Myo10-ΔF2 or GFP-Myo10-ΔF3, fixed and labeled with the membrane dye WGA-Rhodamine. Only GFP-Myo10-ΔF3 is able to create numerous TNTs between cells. Scale bars: 10 μm. (B) The number of transfected cells connected with TNTs was counted. Differently from GFP-Myo10-ΔF2 ($n=280$) both full-length GFP-Myo10 ($n=310$) and GFP-Myo10-ΔF3 ($n=417$) increase the number of TNTs. The level of transfection for these constructs ranges from 35–45% for GFP-Myo10-ΔF2 and 45–55% for GFP-HMM-Myo10. These data are the average of at least three independent experiments. (C) Quantification of the number of TNTs in transfected cells. TNTs between cells were counted, and the numbers of cells with two or less and three or more TNTs were plotted. Full-length GFP-Myo10- and GFP-Myo10-ΔF3- but not GFP-Myo10-ΔF2-expressing cells, are able to form multiple TNTs. Data are the average of at least three independent experiments. (D) The relative percentage of transfer of DiD-labeled vesicles, assessed by flow cytometry, is plotted. GFP-Myo10 and GFP-Myo10-ΔF3 expression in donor cells increases the transfer of DiD-vesicles compared with GFP-vector and GFP-Myo10-ΔF2. These data are the average of five independent experiments. Graphs show means ($\pm$s.e.m.). Overall, these data identify the F2 lobe of the FERM domain as a required component for Myo10-dependent TNT formation in CAD cells. (E) No colocalization of GFP-N-cadherin with mCherry-Myo10 was observed in co-transfected CAD cells. Cells co-transfected with mCherry-Myo10 and GFP-N-cadherin were fixed and imaged. GFP-N-cadherin is rarely found in filopodia and does not colocalize with mCherry-Myo10. Scale bars: 10 μm. *, see Statistical analyses under Materials and Methods; ns, not significant.

and has a specific orientation compared with other FERM subdomains (Wei et al. 2011). Deletion of the F2 lobe could, therefore, disturb the correct orientation and folding of Myo10, thereby affecting cargo recognition (Wei et al., 2011, Hirano 2011). Although most cargoes appear to bind to the F3 lobe, it is conceivable that the F2 lobe interacts with a crucial binding partner that is involved either in the attachment and/or in the fusion of TNTs with the acceptor cells. This would explain why this lobe is not important for dorsal filopodia but necessary for the formation of functional TNTs. Whereas the specific cargoes are still unknown, our data show that, in transfected cells, Myo10

and N-cadherin do not colocalize (Fig. 5E), N-cadherin being a putative Myo10-binding partner (Almagro et al., 2010), which was thought to be involved in TNT formation (Lokar et al., 2010). Our findings suggest that interaction of N-cadherin with Myo10 is not required for TNT formation in CAD cells.

Whether Myo10 is necessary for the initiation of filopodia, or required for the transport of components necessary for actin polymerization at the tips of filopodia, such as VASP or PtdIns(3,4,5)P_3, or whether it helps the growing actin filaments by exerting a direct force at the tips remain to be determined. Importantly, our study suggests that inside the Myo10-dependent
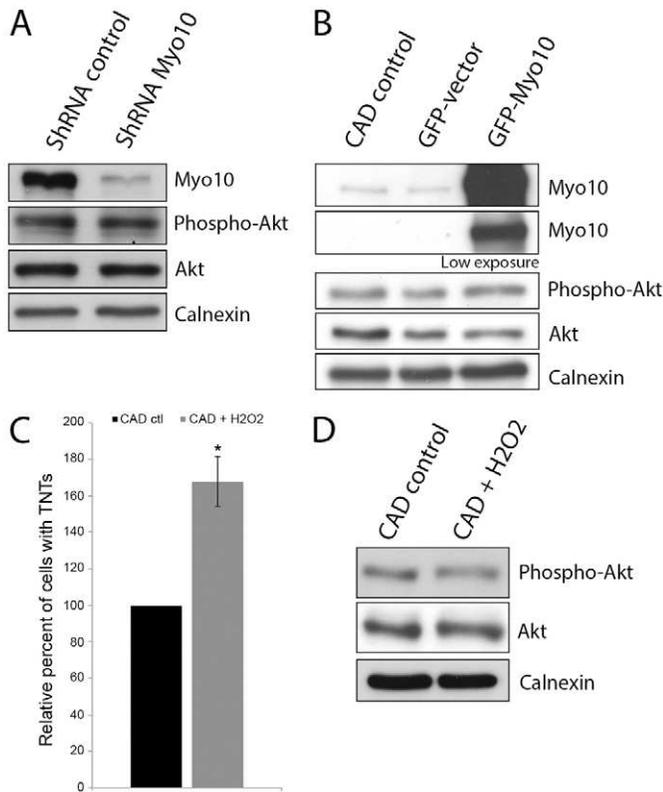
Fig. 6. Similar to Myo10-dependent TNTs, the regulation of TNTs in response to stress in CAD cells is independent of Akt activation. (A) CADs cells downregulated for Myo10 (using Myo10 shRNA lentiviral particles) or control CAD cells (using scramble shRNA lentiviral particles) were plated for 3 days, lysed, and 30 μg of protein was separated on an SDS-PAGE, transferred and subjected to western blotting. As can be seen in the top band, the levels of endogenous Myo10 are downregulated when using the Myo10 shRNA lentiviral particles but, under these conditions, levels of endogenous Akt and phosphorylated Akt (Phospho-Akt) are not affected. (B) Myo10 levels and Akt activation was assessed in non-transfected CAD cells and cells transiently transfected with GFP-vector (controls), and results were compared with those derived from transfected cells expressing GFP-Myo10. The samples were run on a gel and transferred to PVDF membranes for western blot analysis. Overexpression of GFP-Myo10 greatly increases the levels of Myo10 but does not affect the levels of Akt and phosphorylated Akt. (C) Oxidative stress enhances the number of TNT-like structures observed in CAD cells. CAD cells, treated or not (control) with 200 μM of H_2O_2 for 24 hours, were fixed and labeled with WGA-Rhodamine and TNTs were counted 24 hours post-treatment in untreated cells ($n=735$) and in treated cells ($n=588$). Data are the average of three independent experiments (mean ± s.e.m). (D) CAD cells plated for 3 days, were treated with 200 μM of H_2O_2 or no H_2O_2 (control) for 24 hours, washed, lysed and 30 μg of protein was run on an SDS-PAGE, transferred and subjected to western blotting. Treatment of CAD cells with H_2O_2 did not increase the levels of endogenous Akt and phosphorylated Akt. *, see Statistical analyses under Materials and Methods.

TNTs the transfer of vesicle is unidirectional, from the cells that created the tubes towards the recipient cells. This would be consistent with an involvement of Myo10 in promoting the polarized growth of actin cables inside the TNT and/or in vesicle transport. Whether this involves Myo10 directly or requires other myosins needs to be explored. Whereas the specific requirement of the F2 lobe of the FERM domain for TNT formation allows one to discriminate between Myo10-induced dorsal filopodia and TNTs, we also demonstrate that TNTs do not arise from any dorsal

filopodia. Indeed, overexpression of known dorsal filopodia inducers, such as VASP or fascin, failed to promote TNTs (Fig. 1C). Interestingly, in addition to a drastic reduction in the number of TNTs, overexpression of VASP changed the morphology of CAD cells, increasing the cell-to-cell contact zones (Sup. Fig. 1), a fact that is reminiscent to VASP and cadherin-dependent formation of adhesion zippers described in epithelial cells (Vasioukhin et al., 2000).

Downregulation and rescue experiments demonstrated that Myo10 is necessary for the formation of a subset of TNTs and for vesicle transfer (Fig. 3B,C). However, a large number of TNTs remained in Myo10-knockdown cells, along with intercellular transfer of vesicles (Fig. 3B,C). This could be because (1) we were unable to completely silence Myo10 gene expression (Fig. 3A); (2) CAD cells are able to form TNTs after cell-to-cell separation (supplementary material Fig. S1 and Movie 2), a process that might not require Myo10 or (3) Myo10 can enhance *de novo* TNT formation but is not a limiting factor. It is worth noting that similar results were observed with dorsal filopodia, in which 90% gene silencing did not abrogate all dorsal filopodia induction (Bohil et al., 2006), Similarly, downregulation of M-Sec, a protein important for TNT formation in immune cells led to a partial decrease in TNTs, with one-third of the M-Sec-knockdown cells still able to form TNTs (Hase et al., 2009). Finally, a recent article showing the involvement of LST1 in TNT formation (Schiller et al., 2012) found an overall reduction of 46% of cells with TNTs and a 30% decrease of the transfer of vesicles after gene silencing compared with their control cells. Overall, these experiments support the existence of multiple non-redundant mechanisms of TNT formation in the same cell type, possibly induced by different stimuli under different conditions.

Our data also point towards the existence of main differences in the mechanisms of TNT formation in different cell types. We show that, similar to astrocytes (Wang et al., 2011), neuronal cells are able to induce TNT formation as a response to external stress signals such as oxidative stress. However, it appears that the mechanisms of TNT formation are the results of the activation of different signaling pathways in the two cell types. In astrocytes, the main signaling pathway following stress conditions that leads to the formation of TNT is activation of p53 and the Akt/mTOR signaling pathway (Wang et al., 2011). By contrast, we show that in neuronal cells oxidative stress increases TNTs in an Akt-independent manner, and no activation of the Akt pathway in Myo10-overexpressing cells was observed. These data suggest that multiple mechanisms of TNT formation exist, and that different cell types have evolved different ways to form TNTs. However, because Myo10 is expressed in most tissues and different cell types (Berg et al., 2000; Yonezawa et al., 2000), it will be interesting to determine whether it also plays a role in LST1 or mSec-dependent TNT formation or whether its role in TNT formation is restricted to neuronal cells.

In the brain, Myo10 is upregulated during nerve regeneration following sciatic axotomy (Tanabe et al., 2003) or following peripheral nerve injury (Plantman et al., 2013). In addition, Myo10 is highly regulated during development of the nervous system and exists in two forms (Sousa et al., 2006), the full-length and the 'headless' isoform, which lacks the motor activity and is differently regulated during development (Sousa et al., 2006; Raines et al., 2012). Headless myosin is enriched in regions of proliferating and migrating cells (Raines et al., 2012), and was hypothesized to act as a dominant-negative isoform, regulating

Myo10 full-length activity in neurons (Sousa et al., 2006; Zhu et al., 2007; Wang et al. 2009). Consistent with this hypothesis, in cortical neurons, knockdown of full-length Myo10 reduces axon outgrowth, whereas knockdown of headless Myo10 increases axon outgrowth (Raines et al., 2012). In addition, headless Myo10 has been shown to suppress the filopodia-inducing activity of the full-length protein when coexpressed in COS-7 cells (Raines et al., 2012). Here, however, we show that coexpression of both isoforms does not block TNT induction (Fig. 4E), thus highlighting differences in the regulation of Myo10 activity in filopodia and TNTs. Interestingly, in the brain the netrin receptors deleted in colorectal cancer (DCC) and neogenin (NEO1) have different affinities for full-length Myo10 or the short headless form (Zhu et al., 2007). Indeed, whereas both receptors bind to the FERM domain of Myo10, neogenin associates more strongly to the headless form of Myo10 whereas DCC has a greater binding affinity for full-length Myo10. In addition, the expression of DCC but not neogenin stimulates filopodia elongation (Zhu et al., 2007). Thus, the levels of both forms of Myo10 in the brain and their binding to the netrin receptors could be how TNT formation and different downstream signaling pathways in the brain are regulated. The significance of TNTs in the brain is not understood. It is clear that distant cell communication has a main role during development (For review see Abounit et al., 2012). Therefore, the regulation of TNTs by Myo10 expression could have an important role. In addition it was shown that the misfolded infectious prion proteins (PrP^{Sc}) (Gousset et al., 2009; Langevin et al., 2010) and intracellular Aβ-fusion proteins (Wang et al., 2011), as well as the aggregated form of Htt (Huntingtin) exon 1 (Costanzo et al., 2013) take advantage of TNTs for intercellular spread. This suggests that prion diseases and other neurological diseases that occur as the result of protein misfolding, such as Alzheimer, Parkinson and Huntington, use TNTs as a common spreading mechanism (For review see Marzo et al., 2012; Costanzo and Zurzolo, 2013). Interestingly, preliminary data in our laboratory suggest that overexpression of GFP-Myo10 results in a drastic increase in the transfer of PrP^{Sc} particles from chronically infected ScCAD cells to non-infected CAD cells (our unpublished data). Thus, it is possible that, upon stress, toxicity due to prion infection or the presence of toxic aggregates, the levels of full-length Myo10 are upregulated, which leads to an increase in TNT-like structures allowing faster spreading of prions and prion-like proteins in the brain (for a review see Costanzo and Zurzolo, 2013). Studies on the role of toxicity due to infection and/or the presence of aggregates are currently underway in our laboratory.

Overall, this study highlights the key role that Myo10 has in TNT formation within neuronal cells and the differences compared with other cellular models. Further investigation will be necessary to determine the specific role of the F2 lobe of the FERM domain in TNT formation. It is also tempting to speculate that the balance of the levels of full-length and the headless isoform of Myo10 in the brain is a way to regulate TNT formation. Therefore, whether and how these levels vary in cases of brain injuries, toxic stimuli during prion infection or during the progression of neurodegenerative diseases will deserve full attention.

Material and Methods
Cell lines, antibodies, transfection and transduction
Mouse neuronal CAD cells were a gift from Hubert Laude (Institut National de la Recherche Agronomique, Jouy-en-Josas, France) and were cultured in Opti-MEM (Invitrogen) and 10% fetal bovine serum. Transient transfections were performed with Lipofectamine 2000 (Invitrogen) in accordance with the manufacturer's instructions. The bovine GFP-Myo10, GFP-HMM-Myo10 and GFP-Myo10-Headless were gifts from Richard E. Cheney (University of North Carolina, Chapel Hill, NC, USA) and GFP-Myo10-ΔF2, GFP-Myo10-ΔF3, mCherry-Myo10 and mCherry-Myo10-KK1215/6AA (PH2 mutant) were gifts from Staffan Strömblad (Center for Biosciences, Department of Biosciences and Nutrition, Karolinska Institutet, Stockholm, Sweden). GFP-Fascin was a gift from Josephine C. Adams (Dept. of Cell Biology, Cleveland Clinic, Cleveland, USA) and GFP-VASP was obtained from Sandrine Etienne-Manneville (Pasteur Institute, Paris, France). Human anti-Myo10 rabbit polyclonal antibody, which detects Myo10 from multiple species including mouse, was purchased from Sigma (HPA024223) and Myo10 shRNA lentiviral particles, control shRNA lentiviral particles and Polybrene® reagent were from Santa Cruz Biotechnology, Inc., and were used according to the manufacturer's instructions. Akt and Phospo-Akt antibodies were purchased from Cell Signaling Technology, Inc. and wheat germ agglutinin (WGA) tetramethylrhodamine conjugate (WGA-Rhodamine) and the lipophilic dye DiD were purchased from Molecular Probes (Invitrogen). Hydrogen peroxide (30% wt) was purchased from Sigma.

Myo10 shRNA lentiviral particle transduction and selection of stable clones
CAD cells were plated at a density of 40,000 in a 12-well plate for 24 hours before transduction. Transduction was performed according to the manufacturers' instructions (Santa Cruz Biotechnology, Inc). Stable clones that express both control Myo10 and Myo10 short hairpin RNA (shRNA) were selected, and maintained in culture by adding 5 μg/ml of puromycin dihydrochloride to eliminate non-transduced cells. Western blotting was used to evaluate downregulation of gene expression and to select for the best clones.

For rescue experiments, stable shRNA control and shRNA-Myo10 cells were transfected with GFP-vector or GFP-Myo10, respectively, using Lipofectamine 2000. Twenty-four hours after transfection, TNTs were counted in cells or for flow-cytometry analyses was carried out as described below.

Because the Myo10 shRNA lentiviral particles that we used in our experiments had been designed to inhibit expression of Myo10 in mouse cells and we used a bovine GFP-Myo10 construct for transient transfections, the construct was not a target for shRNA and normal expression levels were observed.

Gel electrophoresis and western blots
Transfected cells, shRNA knockdown cells or cells treated with H$_2$O$_2$ (200 μM for 24 hours) were lysed in lysis buffer (0,5% Triton X-100, 0,5% DOC, 100 mM NaCl, 10 mM Tris-HCl pH 8) and the amount of protein per μl was quantified in a Bradford assay. Thirty micrograms of protein, denatured in Laemmli buffer and boiled for 5 minutes, was loaded on 8% SDS-polyacrylamide gels and transferred into PVDF membrane for western blot analyses with the appropriate primary antibodies. HRP-conjugated secondary antibodies and ECL^{TM} reagents from Amersham (GE Healthcare) were used for detection.

Detection of TNTs by using fluorescence microscopy
To evaluate the number of TNT-connected cells, TNTs were analyzed by fluorescence microscopy. Cells were plated on T25 flasks overnight and transfected the following day with the appropriate plasmids using Lipofectamine 2000. The next day, cells were counted and 200,000 cells were plated overnight on Ibidi μ-Dishes (Biovalley, France) at 37℃. Cells were then fixed for 20 minutes at room temperature (RT) using fixative solution 1 (2% PFA, 0.05% glutaraldehyde and 0.2 M HEPES in PBS) followed by an additional incubation of 20 minutes with fixative solution 2 (4% PFA and 0.2 M HEPES in PBS). The cells were carefully washed in PBS and labeled for 20 minutes at RT with WGA-Rhodamine (1:300 in PBS), washed and sealed with Aqua-Poly mount (Polysciences, Inc.). Image stacks covering the whole cellular volume were acquired using a widefield microscope (Zeiss Axiovert 200M) controlled by Axiovision software. To evaluate the number of TNT-connected cells (i.e. structures connecting two cells that do not touch the substratum), manual analysis was performed and each experiment was carried out at least in triplicate. Image analyses of raw data, such as Z-projections and 3D reconstructions, were obtained using ImageJ software (http://rsb.info.nih.gov/ij/) and OsiriX (Osirix Medical Imaging software) software programs.

Live imaging systems
The membrane of CAD cells was labeled with 5-carboxytetramethylrhodamine succinimidyl-ester for 1 hour at 37℃, and cells were imaged live using an Andor spinning-disk confocal microscope. Z-stacks of 0.3 μm steps were taken for each time point and Z-projections were obtained in order to look at filopodia-driven TNT formation over time (Movie 1). The same imaging system was used to analyze the movements of GFP-Myo10 within TNTs in transiently transfected CAD cells over specific periods of time (supplementary material Movie 3). Long time-lapse movies were acquired with the Biostation IM from Nikon (Movie 2). Image analyses of raw data was obtained using ImageJ (http://rsb.info.nih.gov/ij/) software program.

Flow cytometry assay to quantify the transfer of DiD-labeled vesicles

CAD cells were transfected with the appropriate GFP-constructs (donor cells) and CFP-vector (acceptor cells) in T25 dishes for 24 hours. The donor cells were then counted and labeled with the membrane dye DiD (1:3000 in complete medium for 30 minutes at 37℃), the cells were centrifuged at 1000 rpm for 5 minutes, to remove the DiD solution, resuspended in complete medium and incubated for 30 more minutes at 37℃ (to internalize the dye). The cells were then centrifuged once more to wash away any remaining dye. The labeled donor cells were then mixed (1:1) with CFP-transfected acceptor cells and plated on 35-mm dishes overnight. Each independent experiment was performed in triplicates. The following day, cells were washed with PBS to remove any dead cells, scraped of the dishes with 500 μl PBS and passed through sterile 40-μm nylon cell strainers (BD Falcon^{TM}) in order to obtain single-cell suspensions. Cells were then mixed with 500 μl of 4% PFA (2% final solution). For FACS analyses, DiD-labeled donor cells and CFP-vector-transfected acceptor cells were analyzed at 633 nm and 488 nm excitation wavelengths, respectively. Flow cytometry data were acquired using a CyAn ADP flow cytometer (Dako Cytomation, Beckman Coulter, Inc.). Samples were analyzed at low flow rate, corresponding to 50–150 events per second, and each independent experiment was performed in triplicate (30,000 cells for each condition). Doublet discrimination on the basis of signal processing was achieved by plotting the peak height against the area of side scatter. The data were analyzed using Kaluza® Flow Analysis Software (Beckman Coulter, Inc.).

Statistical analyses

In order to analyze the significance between two experimental conditions, we used the Mann-Whitney U-Test. The z-score was calculated using the normal approximation, such that $z = \dfrac{U - \dfrac{n_x n_y}{2}}{\sqrt{\dfrac{n_x n_y (N+1)}{12}}}$.

The differences were considered significant at *$P<0.05$ when $-1.96>z>1.96$; at **$P<0.01$ when $-2.58>z>2.58$; or ***$P<0.001$ when $-3.291>z>3.291$, where z is the z-score for the normal approximation of the data. In graphs, asterisks above columns indicate comparison with control cells, whereas brackets indicate any other paired comparisons.

Author Contributions

C.Z. coordinated the project. K.G. planned, performed and analyzed the experiments. L.M. performed the unpublished infectious experiments and provided technical help. P.-H.C. set up the parameters for the flow cytometry assays. K.G. and C.Z. wrote the manuscript. All authors discussed the results and manuscript text.

Competing Interests

The authors declare that they have no competing interests.

Supplementary material available online at
http://jcs.biologists.org/lookup/suppl/doi:10.1242/jcs.129239/-/DC1

References

Abounit, S. and Zurzolo, C. (2012). Wiring through tunneling nanotubes – from electrical signals to organelle transfer. *J. Cell Sci.* **125**, 1089-1098.

Adams, J. C. and Schwartz, M. A. (2000). Stimulation of fascin spikes by thrombospondin-1 is mediated by the GTPases Rac and Cdc42. *J. Cell Biol.* **150**, 807-822.

Almagro, S., Durmort, C., Chervin-Pétinot, A., Heyraud, S., Dubois, M., Lambert, O., Maillefaud, C., Hewat, E., Schaal, J. P., Huber, P. and Gulino-Debrac, D. (2010). The motor protein myosin-X transports VE-cadherin along filopodia to allow the formation of early endothelial cell-cell contacts. *Mol. Cell Biol.* **7**, 1703-1717.

Berg, J. S. and Cheney, R. E. (2002). Myosin-X is an unconventional myosin that undergoes intrafilopodial motility. *Nat. Cell Biol.* **4**, 246-250.

Berg, J. S., Derfler, B. H., Pennisi, C. M., Corey, D. P. and Cheney, R. E. (2000). Myosin-X, a novel myosin with pleckstrin homology domains, associates with regions of dynamic actin. *J. Cell Sci.* **113**, 3439-3451.

Bohil, A. B., Robertson, B. W. and Cheney, R. E. (2006). Myosin-X is a molecular motor that functions in filopodia formation. *Proc. Natl. Acad. Sci. USA* **103**, 12411-12416.

Bukoreshtliev, N. V., Wang, X., Hodneland, E., Gurke, S., Barroso, J. F. and Gerdes, H. H. (2009). Selective block of tunneling nanotube (TNT) formation inhibits intercellular organelle transfer between PC12 cells. *FEBS Lett.* **583**, 1481-1488.

Costanzo, M. and Zurzolo, C. (2013). The cell biology of prion-like spread of protein aggregates: mechanisms and implication in neurodegeneration. *Biochem. J.* **452**, 1-17.

Costanzo, M., Abounit, S., Marzo, L., Danckaert, A., Chamoun, Z., Roux, P. and Zurzolo, C. (2013). Transfer of polyglutamine aggregates in neuronal cells occurs in tunneling nanotubes. *J. Cell Sci.* **126**, 3678-3685.

Davis, D. M. and Sowinski, S. (2008). Membrane nanotubes: dynamic long-distance connections between animal cells. *Nat. Rev. Mol. Cell Biol.* **9**, 431-436.

Eugenin, E. A., Gaskill, P. J. and Berman, J. W. (2009). Tunneling nanotubes (TNT) are induced by HIV-infection of macrophages: a potential mechanism for intercellular HIV trafficking. *Cell. Immunol.* **254**, 142-148.

Gousset, K., Schiff, E., Langevin, C., Marijanovic, Z., Caputo, A., Browman, D. T., Chenouard, N., de Chaumont, F., Martino, A., Enninga, J. et al. (2009). Prions hijack tunnelling nanotubes for intercellular spread. *Nat. Cell Biol.* **11**, 328-336.

Gurke, S., Barroso, J. F., Hodneland, E., Bukoreshtliev, N. V., Schlicker, O. and Gerdes, H. H. (2008). Tunneling nanotube (TNT)-like structures facilitate a constitutive, actomyosin-dependent exchange of endocytic organelles between normal rat kidney cells. *Exp. Cell Res.* **314**, 3669-3683.

Hase, K., Kimura, S., Takatsu, H., Ohmae, M., Kawano, S., Kitamura, H., Ito, M., Watarai, H., Hazelett, C. C., Yeaman, C. et al. (2009). M-Sec promotes membrane nanotube formation by interacting with Ral and the exocyst complex. *Nat. Cell Biol.* **11**, 1427-1432.

Hirano, Y., Hatano, T., Takahashi, A., Toriyama, M., Inagaki, N. and Hakoshima, T. (2011). Structural basis of cargo recognition by the myosin-X MyTH4-FERM domain. *EMBO J.* **30**, 2734-2747.

Kerber, M. L. and Cheney, R. E. (2011). Myosin-X: a MyTH-FERM myosin at the tips of filopodia. *J. Cell Sci.* **124**, 3733-3741.

Langevin, C., Gousset, K., Costanzo, M., Richard-Le Goff, O. and Zurzolo. (2010). Characterization of the role of dendritic cells in prion transfer to primary neurons. *Biochem. J.* **431**, 189-198.

Lokar, M., Iglic, A. and Veranic, P. (2010). Protruding membrane nanotubes: attachment of tubular protrusions to adjacent cells by several anchoring junctions. *Protoplasma* **246**, 81-87.

Marzo, L., Gousset, K. and Zurzolo, C. (2012). Multifaceted roles of tunneling nanotubes in intercellular communication. *Front. Physiol* **3**, 72.

Onfelt, B., Nedvetzki, S., Yanagi, K. and Davis, D. M. (2004). Cutting edge: membrane nanotubes connect immune cells. *J. Immunol.* **173**, 1511-1513.

Onfelt, B., Nedvetzki, S., Benninger, R. K., Purbhoo, M. A., Sowinski, S., Hume, A. N., Seabra, M. C., Neil, M. A., French, P. M. and Davis, D. M. (2006). Structurally distinct membrane nanotubes between human macrophages support long-distance vesicular traffic or surfing of bacteria. *J. Immunol.* **177**, 8476-8483.

Pasquier, J., Guerrouahen, B. S., Al Thawadi, H., Ghiabi, P., Maleki, M., Abu-Kaoud, N., Jacob, A., Mirshahi, M., Galas, L., Rafii, S. et al. (2013). Preferential transfer of mitochondria from endothelial to cancer cells through tunneling nanotubes modulates chemoresistance. *J. Transl. Med.* **11**, 94. (Epub ahead of print).

Plantard, L., Arjonen, A., Lock, J. G., Nurani, G., Ivaska, J. and Strömblad, S. (2010). PtdIns(3,4,5)P$_3$ is a regulator of myosin-X localization and filopodia formation. *J. Cell Sci.* **123**, 3525-3534.

Plantman, S., Zelano, J., Novikova, L. N., Novikov, L. N. and Cullheim, S. (2013). Neuronal myosin-X is upregulated after peripheral nerve injury and mediates laminin-induced growth of neurites. *Mol. Cell. Neurosci.* **56**, 96-101.

Qi, Y., Wang, J. K., McMillian, M. and Chikaraishi, D. M. (1997). Characterization of a CNS cell line, CAD, in which morphological differentiation is initiated by serum deprivation. *J. Neurosci.* **17**, 1217-1225.

Raines, A. N., Nagdas, S., Kerber, M. L. and Cheney, R. E. (2012). Headless Myo10 is a negative regulator of full-length Myo10 and inhibits axon outgrowth in cortical neurons. *J. Biol. Chem.* **287**, 24873-24883.

Rustom, A., Saffrich, R., Markovic, I., Walther, P. and Gerdes, H. H. (2004). Nanotubular highways for intercellular organelle transport. *Science* **303**, 1007-1010.

Schiller, C., Diakopoulos, K. N., Rohwedder, I., Kremmer, E., von Toerne, C., Ueffing, M., Weidle, U. H., Ohno, H. and Weiss, E. H. (2013). LST1 promotes the assembly of a molecular machinery responsible for tunneling nanotube formation. *J. Cell Sci.* **126**, 767-777.

Sousa, A. D., Berg, J. S., Robertson, B. W., Meeker, R. B. and Cheney, R. E. (2006). Myo10 in brain: developmental regulation, identification of a headless isoform and dynamics in neurons. *J. Cell Sci.* **119**, 184-194.

Sowinski, S., Jolly, C., Berninghausen, O., Purbhoo, M. A., Chauveau, A., Köhler, K., Oddos, S., Eissmann, P., Brodsky, F. M., Hopkins, C. et al. (2008). Membrane nanotubes physically connect T cells over long distances presenting a novel route for HIV-1 transmission. *Nat. Cell Biol.* **10**, 211-219.

Tanabe, K., Bonilla, I., Winkles, J. A. and Strittmatter, S. M. (2003). Fibroblast growth factor-inducible-14 is induced in axotomized neurons and promotes neurite outgrowth. *J. Neurosci.* **23**, 9675-9686.

Tokuo, H., Mabuchi, K. and Ikebe, M. (2007). The motor activity of myosin-X promotes actin fiber convergence at the cell periphery to initiate filopodia formation. *J. Cell Biol.* **179**, 229-238.

Umeki, N., Jung, H. S., Sakai, T., Sato, O., Ikebe, R. and Ikebe, M. (2011). Phospholipid-dependent regulation of the motor activity of myosin X. *Nat. Struct. Mol. Biol.* **18**, 783-788.

Van Prooyen, N., Gold, H., Andresen, V., Schwartz, O., Jones, K., Ruscetti, F., Lockett, S., Gudla, P., Venzon, D. and Franchini, G. (2010). Human T-cell leukemia virus type 1 p8 protein increases cellular conduits and virus transmission. *Proc. Natl. Acad. Sci. USA* **107**, 20738-20743.

Vasioukhin, V., Bauer, C., Yin, M. and Fuchs, E. (2000). Directed actin polymerization is the driving force for epithelial cell-cell adhesion. *Cell* **100**, 209-219.

Wang, J. J., Fu, X. Q., Guo, Y. G., Yuan, L., Gao, Q. Q., Yu, H. L., Shi, H. L., Wang, X. Z., Xiong, W. C. and Zhu, X. J. (2009). Involvement of headless myosin X in the motility of immortalized gonadotropin-releasing hormone neuronal cells. *Cell Biol. Int.* **33**, 578-585.

Wang, X., Veruki, M. L., Bukoreshtliev, N. V., Hartveit, E. and Gerdes, H. H. (2010). Animal cells connected by nanotubes can be electrically coupled through interposed gap-junction channels. *Proc. Natl. Acad. Sci. USA* **107**, 17194-17199.

Wang, Y., Cui, J., Sun, X. and Zhang, Y. (2011). Tunneling-nanotube development in astrocytes depends on p53 activation. *Cell Death Differ.* **18**, 732-742.

Watanabe, T. M., Tokuo, H., Gonda, K., Higuchi, H. and Ikebe, M. (2010). Myosin-X induces filopodia by multiple elongation mechanism. *J. Biol. Chem.* **285**, 19605-19614.

Watkins, S. C. and Salter, R. D. (2005). Functional connectivity between immune cells mediated by tunneling nanotubes. *Immunity* **23**, 309-318.

Weber, K. L., Sokac, A. M., Berg, J. S., Cheney, R. E. and Bement, W. M. (2004). A microtubule-binding myosin required for nuclear anchoring and spindle assembly. *Nature* **431**, 325-329.

Wei, Z., Yan, J., Lu, Q., Pan, L. and Zhang, M. (2011). Cargo recognition mechanism of myosin X revealed by the structure of its tail MyTH4-FERM tandem in complex with the DCC P3 domain. *Proc. Natl. Acad. Sci. USA* **108**, 3572-3577.

Yonezawa, S., Kimura, A., Koshiba, S., Masaki, S., Ono, T., Hanai, A., Sonta, S., Kageyama, T., Takahashi, T. and Moriyama, A. (2000). Mouse myosin X: molecular architecture and tissue expression as revealed by northern blot and in situ hybridization analyses. *Biochem. Biophys. Res. Commun.* **271**, 526-533.

Yoshizaki, T., Imamura, T., Babendure, J. L., Lu, J. C., Sonoda, N. and Olefsky, J. M. (2011). Myosin 5a is an insulin-stimulated Akt2 (protein kinase Bbeta) substrate modulating GLUT4 vesicle translocation. *Mol. Cell Biol.* **27**, 5172-5183.

Zhang, H., Berg, J. S., Li, Z., Wang, Y., Lång, P., Sousa, A. D., Bhaskar, A., Cheney, R. E. and Strömblad, S. (2004). Myosin-X provides a motor-based link between integrins and the cytoskeleton. *Nat. Cell Biol.* **6**, 523-531.

Zhu, X. J., Wang, C. Z., Dai, P. G., Xie, Y., Song, N. N., Liu, Y., Du, Q. S., Mei, L., Ding, Y. Q. and Xiong, W. C. (2007). Myosin X regulates netrin receptors and functions in axonal path-finding. *Nat. Cell Biol.* **9**, 184-192.